Amphiphiles

Deutsche Ausgabe: DOI: 10.1002/ange.201506493
Internationale Ausgabe: DOI: 10.1002/anie.201506493

Loading of Vesicles into Soft Amphiphilic Nanotubes using Osmosis

*Petra M. Erne, Laura S. van Bezouwen, Peter Štacko, Derk Jan van Dijken, Jiawen Chen, Marc C. A. Stuart, Egbert J. Boekema, and Ben L. Feringa**

Abstract: *The facile assembly of higher-order nanoarchitectures from simple building blocks is demonstrated by the loading of vesicles into soft amphiphilic nanotubes using osmosis. The nanotubes are constructed from rigid interdigitated bilayers which are capped with vesicles comprising phospholipid-based flexible bilayers. When a hyperosmotic gradient is applied to these vesicle-capped nanotubes, the closed system loses water and the more flexible vesicle bilayer is pulled inwards. This leads to inclusion of vesicles inside the nanotubes without affecting the tube structure, showing controlled reorganization of the self-assembled multicomponent system upon a simple osmotic stimulus.*

Pushing the boundaries of chemical self-assembly continues to present important challenges to the field of dynamic molecular systems and nanoscience.[1] Self-assembled systems can be obtained from a variety of components including nanoparticles, small molecules, and polymers.[2] The construction of higher-order architectures requires the use of building blocks that can co-assemble in distinct functional units.[3] A particularly promising approach resides in the design and application of orthogonal amphiphilic structures.[4] As well as the use of a large variety of naturally-occurring amphiphiles,[5] major effort has been devoted to the synthesis of novel amphiphilic molecules which can self-assemble into nanotubes, vesicles, ribbons, sheets, or helical structures.[6] Prominent examples include amphiphilic polymers[7] and block copolymers,[8] amphiphilic peptides,[9] and photoresponsive amphiphiles.[10]

Furthermore, particular focus has been directed toward the development of multicomponent[11] and stimuli-responsive[12] self-assembled systems which adapt in response to light,[13] temperature,[14] magnetic,[15] and electric fields,[16] ionic strength,[17] pH changes,[18] and ultrasound.[19] These stimuli have been explored extensively to induce structural changes in nanostructures, such as nanoparticles,[20] polymers,[21] gels,[22] and porous materials.[23] The inherent ability of a responsive nanoscale architecture to be addressed by an external stimulus makes it attractive for a wide range of applications including, but not limited to, targeted drug delivery,[24] change of the wettability of a surface,[25] biosensing,[26] and other biomedical applications.[27]

However, limited attention has been paid to osmosis as a stimulus for manipulating self-assembled structures[28,29] which is surprising since osmosis is a common regulatory phenomenon in biological systems.[30] To create multicomponent self-assembled systems responsive to osmosis at the nanometer scale, we envisioned to employ the inherent responsive nature of amphiphilic aggregates to osmotic conditions. It is well known that cellular membranes[31] and phospholipid vesicles can change shape[32] after exposure to osmotic conditions.[33] This feature has recently been applied to generate responsive polymer membrane capsules[28] as well as polymersome vesicles.[29] In these cases, a change of the vesicles comparable to phospholipid vesicles under osmotic pressure was detected, that is, the osmotic pressure induced a shape change from a spherical structure to a deflated geometry which can resemble the shape of a red blood cell[34] and is often referred to as a stomatocyte.[32] We consider osmosis an attractive control modality, since a concentration gradient might be employed to facilitate a precise change in the architecture of the self-assembled multicomponent structure. Such a structure should contain semipermeable membranes which are either permeable for the solvent or a solute, for example, ions. In contrast to other stimuli, osmosis is inherently simple, robust, and general, and is therefore an appealing tool to modify self-assembled structures at the nano/micro scale.

In our previous studies,[35] it was shown that amphiphile **1** (Figure 1 A) can assemble, in the presence of 1,2-dioleoyl-*sn*-glycero-3-phosphocholine (DOPC), into vesicle-capped nanotubes which have a uniform diameter of 28 nm. The bilayer thickness for the nanotube is 3 nm and the bilayer dimension of the vesicle cap is 4 nm. The smaller bilayer thickness of the nanotubes was attributed to the fact that the hydrophobic tails of amphiphile **1** interdigitate, maximizing van der Waals interactions which results in the formation of a rigid and stable bilayer, as demonstrated by experiments using the nonionic surfactant Triton X100. In contrast to the DOPC vesicle caps which are disassembled, the nanotubes remain intact upon treatment with Triton X-100, indicating the robustness of the tube bilayer.

We report herein the osmosis-induced change in the shape of nanotube-attached vesicles as a versatile method to encapsulate these vesicles into the nanotube, creating small separate compartments within the nanotube (Figure 1 A). This method is a novel way of using a physically and biologically relevant phenomenon to facilitate the creation of a more complex soft nanostructure. In contrast to other studies where a shape change of vesicle formed by a synthetic

[*] P. M. Erne, P. Štacko, Dr. D. J. van Dijken, Dr. J. Chen, Dr. M. C. A. Stuart, Prof. Dr. B. L. Feringa
Centre for Systems Chemistry
Stratingh Institute for Chemistry, University of Groningen
Nijenborgh 4, 9747 AG, Groningen (The Netherlands)
E-mail: b.l.feringa@rug.nl

L. S. van Bezouwen, Dr. M. C. A. Stuart, Prof. Dr. E. J. Boekema
Electron Microscopy Group, Groningen Biomolecular Sciences and Biotechnology Institute, University of Groningen
Nijenborgh 7, 9747 AG Groningen (The Netherlands)

Supporting information for this article is available on the WWW under http://dx.doi.org/10.1002/anie.201506493.

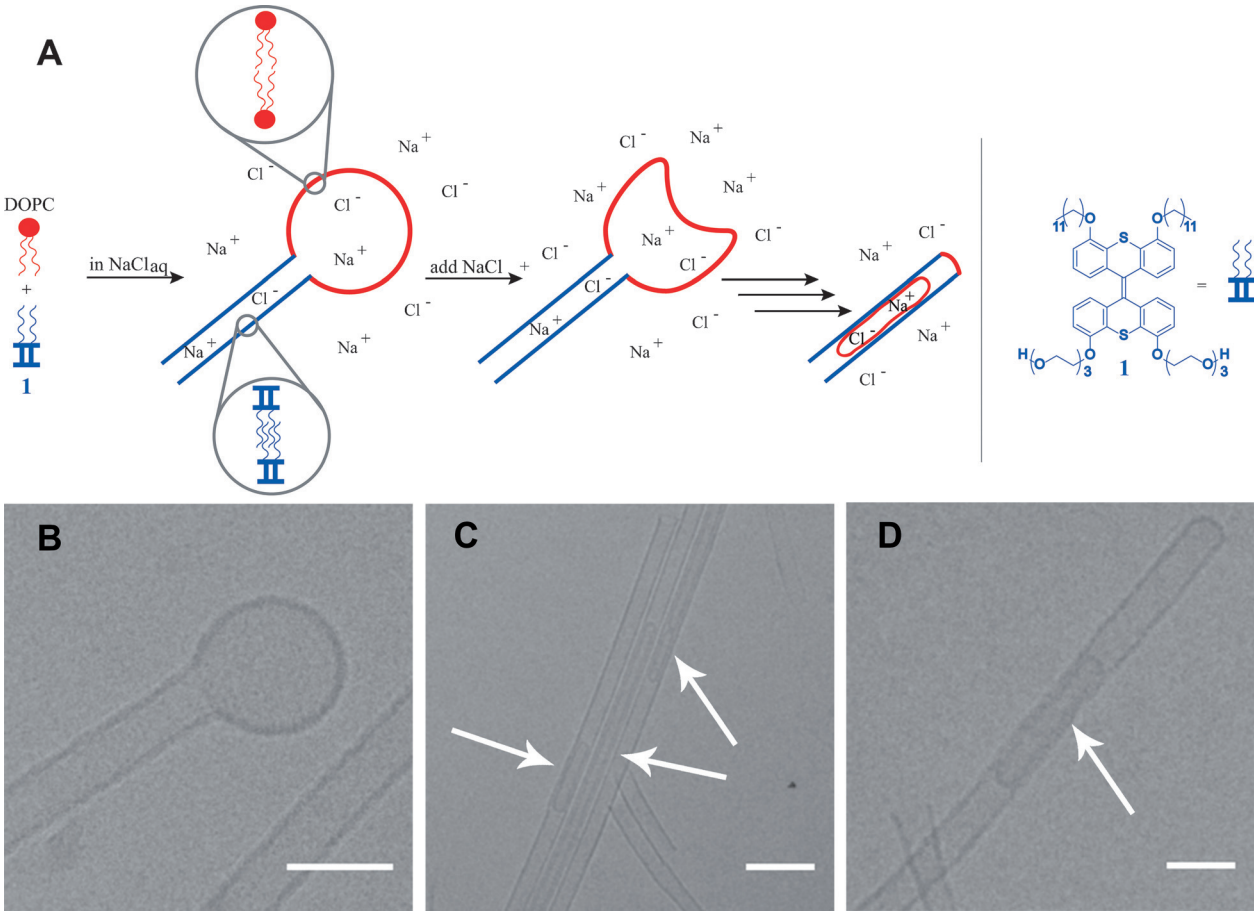

Figure 1. A) Schematic depiction of the inclusion of vesicles into soft amphiphilic nanotubes. The membrane of the DOPC cap is shown in red and the membrane of the nanotube in blue. Upon inducing osmotic pressure by adding NaCl to the outside of the nanotube, water migrates out of the end-capped nanotube causing deformation of the vesicle cap. The inherent rigidity of **1** limits its flexibility upon increased osmotic stress which will cause the inclusion of the DOPC vesicles. B) CryoTEM image of DOPC:**1** (1:1; 1 mg mL^{-1} each) in 10 mM aq. NaCl solution showing an end-capped nanotube. C) CryoTEM image of DOPC:**1** (1:1; 1 mg mL^{-1} each) in 10 mM aq. NaCl solution after addition of a 20 mM aq. NaCl solution showing the inclusion of DOPC vesicles (white arrows). D) CryoTEM image of DOPC:**1** (1:1; 1 mg mL^{-1} each) in 10 mM aq. NaCl after addition of a 40 mM aq. NaCl solution showing the inclusion of DOPC vesicles (white arrow). Scale bars: (B, D) = 50 nm, (C) = 100 nm.

amphiphile was observed upon application of osmotic pressure,[28,29] we not only induce a change in the shape of the vesicle attached to the end of the nanotube under osmotic conditions but use this shape transformation in combination with a geometrically restrictive environment, namely the rigid nanotube to which the vesicle is attached, to create a novel and unprecedented hybrid nanostructure. It should be noted that Shimizu and co-workers[36] observed the formation of tubes with widths of 1–3 μm containing vesicles where both the vesicles and tubes were composed of the same oligoglycine-based bola-amphiphile. In contrast to the multicomponent system presented herein, no osmotic pressure was applied to obtain these structures nor was a shape transformation of the vesicles to a cylindrical shape inside the microtubes observed.

To examine the behavior of the end-capped nanotubes under osmotic conditions, samples of end-capped nanotubes were prepared from a mixture of amphiphile **1** and DOPC in a ratio of 1:1 in a concentration of 1 mg mL^{-1} for each component in an aqueous 10 mM NaCl solution. To induce osmotic pressure, a solution of 20 or 40 mM aqueous NaCl was added in a volumetric ratio of 5:1 resulting in a final concentration of 12 or 15 mM of NaCl "outside" the end-capped nanotubes (see the Supporting Information for all experimental conditions). Under these hyperosmotic conditions, the presence of vesicles inside the nanotubes could be observed by cryoTEM (Figure 1 C and D). The structure of the tube remains intact while an additional cylindrical bilayer structure with a bilayer distinct from the nanotube bilayer is found inside the nanotube. We could observe varying lengths of the cylindrical vesicles inside the nanotubes with sizes ranging from 50 nm up to several hundreds of nanometers which appear to correlate with the initial size of the corresponding vesicles capped at the end of the nanotube (see Section S1 in the Supporting Information). At the same time some small vesicle caps remain at the end of the nanotubes (see below; Figure 3). Furthermore, it has to be noted that both in water and an aqueous salt solution end-capped nanotubes can be observed by cryoTEM (Figure 1 B; Figure S1 in the Supporting Information). The presence of NaCl during the formation of the nanotubes has no significant impact on the nanotubes formed. Therefore, the presence of

salt during the formation of the nanotubes can be ruled out as a cause for the formation of vesicles inside the nanotubes.

Increasing the concentration gradient (the respective NaCl concentrations used outside the nanotubes are 25 mM and 42 mM; see the Supporting Information, materials and methods section for experimental details) between the inside and the outside of the nanotube revealed that even with increasing osmotic pressure small vesicles (below 30 nm in diameter) remained attached as caps to the ends of the nanotubes (Figure S3). This can be attributed to the fact that the stress induced on a membrane while being deformed by osmotic pressure, because of a very high curvature of the bilayer, would be too large and would not allow for the necessary shape transformation required for the small vesicle to be taken into the nanotube.[37] In all cases, vesicles inside the nanotube could be observed (Figure S2–S5).

Electron cryotomography[38] was used to provide further experimental support that the vesicles are located inside the nanotubes (see the Supporting Information, materials and methods section for experimental details). A sample containing nanotubes loaded with vesicles was analyzed by electron cryotomography where a series of TEM images were recorded at various tilt angles. In the region of interest (Figure 2A, marked with a circle) a nanotube with several small vesicles inside is analyzed. In the tomographic slice[39] of the 3D reconstruction (Figure 2B), the DOPC vesicles inside the nanotube are highlighted in red whereas the nanotube bilayer is highlighted in a transparent blue (Figure 2C).[40] Viewing the region of interest from a suitable angle in the 3D reconstruction (Figure 2D) shows that the vesicles are surrounded by the nanotube bilayer which demonstrates that the vesicles are indeed located inside the nanotube. If the capped vesicle was simply changing from a spherical shape into a cylindrical shape while located along the nanotube adapting to osmotic conditions, changing the viewing angle in the 3D reconstruction would readily reveal a geometry where the vesicles are located outside the nanotube.

We anticipate that a possible mechanism for this unprecedented inclusion of vesicles into nanotubes might rely on differences in rigidity between the bilayer of the nanotube and the vesicle. The unique nature and, in particular, the stability of the rigid amphiphilic nanotube connected to a more flexible phospholipid vesicle at its end allows for this specific transformation of a multicomponent self-assembled structure at the nanoscale (Figure 1A). When increasing the salt concentration outside the nanotube, water permeates the bilayers from the inside of the end-capped nanotubes to the outside to equilibrate the salt concentration on both sides of the bilayers. The loss of water results in the deformation of the more flexible vesicle bilayer (Figure 1A) in accordance with previously reported distortion of vesicles under osmotic conditions.[33] Upon further loss of water, the only possible space for the shrinking vesicle is the inside of the nanotube which itself, due to its more rigid bilayer, does not change shape. Finally the vesicle ruptures from the end of the nanotube and is found completely inside the nanotube (Figure 1A; Section S2 in the Supporting Information).

Further support for our proposed mechanism is provided by electron cryotomography, through which we were able to visualize a possible intermediate structure for the proposed inclusion of the vesicles into nanotubes. In the region of interest (Figure 3A), a shape transformation of a vesicle attached to the end of a nanotube into a dented spherical shape which remains attached to the end of the nanotube is evident (Figure 3B, C; black arrow). Additionally, a nanotube with a vesicle inside is also observed (Figure 3B, C; white arrow). Viewing the region of interest at a suitable different angle (Figure 3D) nicely shows the so-called stomatocyte shape of the vesicle capped to the end of the nanotube. This stomatocyte-shaped vesicle is an expected intermediate

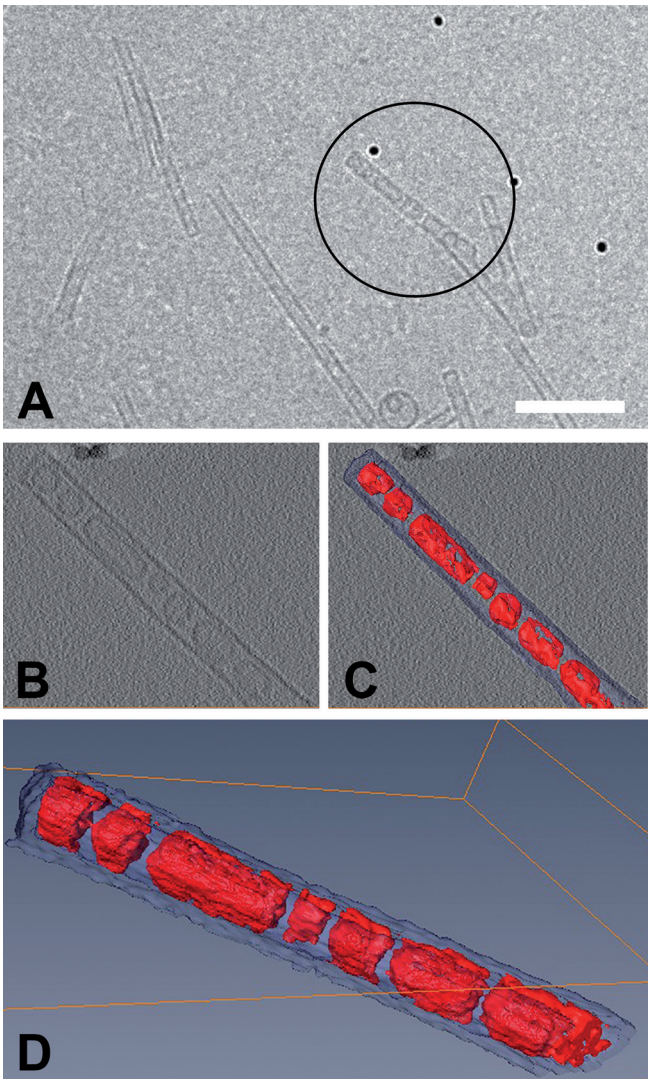

Figure 2. A) CryoTEM image of a sample DOPC:**1** (1:1; 1 mg mL^{-1} each) in 10 mM aq. NaCl after addition of a 200 mM aq. NaCl solution with several DOPC vesicles inside the nanotube. The region of interest is marked with a circle (scale bar = 200 nm). The small black spherical objects are fiducial gold markers. B) Tomographic slice of 3D reconstructed area obtained by electron cryotomography where both the nanotubes and the vesicles inside the nanotube are clearly visible. C) The same region of the reconstructed area (tomographic slice visible in the background) with the surface of the enclosed vesicles colored red and the surface of the nanotube colored transparent blue. D) Same region as in (B) and (C) shown in a 3D reconstruction at a different viewing angle with the same color scheme as in (C).

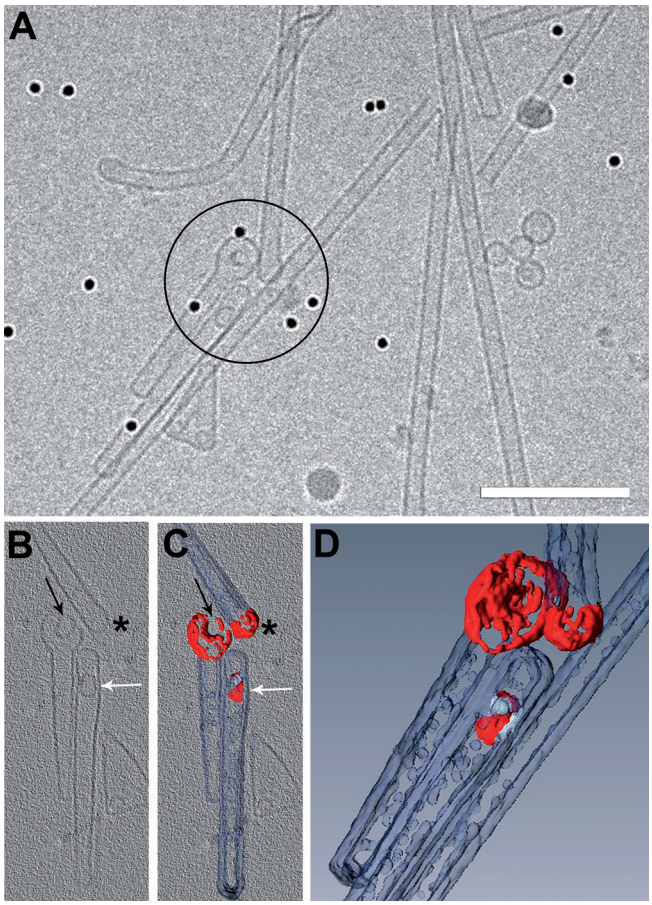

Figure 3. A) CryoTEM of a sample DOPC:**1** (1:1; 1 mg mL^{-1} each) in 10 mM aq. NaCl after addition of 200 mM aq. NaCl solution where the region of interest is highlighted with a circle (scale bar = 200 nm). The small black spherical objects are fiducial gold markers. B) Tomographic slice of reconstructed 3D area obtained by electron cryotomography. C) The same region of the reconstructed area (tomographic slice visible in the background) with the surface of the enclosed vesicles colored red and the surface of the nanotubes colored transparent blue. In both (B) and (C), the progress of inclusion of vesicles into nanotubes from the initially end-capped tube (*), through distorted vesicles attached to the end of a nanotubes (black arrow), to an included vesicle present inside a nanotube (white arrow), is shown. D) The same region as in (B) and (C) shown in a 3D reconstruction at a different viewing angle using the color scheme of (C), showing the dented geometry of the vesicle capping the end of the nanotube.

structure if the osmotic pressure and the resulting effect on the morphology of the vesicles is the driving force for the obtained vesicles inside the nanotube.

Finally we performed studies on the photochemical disassembly of the vesicle-containing nanotubes which showed that the vesicles inside the nanotubes can be released upon irradiation with UV light. Here we take advantage of the unique photoresponsive nature of the bis-thioxanthylidene core unit[41] of the amphiphile that forms the bilayer of the self-assembled nanotube. Upon irradiation with UV light ($\lambda = 365$ nm), we expected that initially nicks and subsequently holes in the walls of the nanotubes would form as a result of irreversible cyclization of **1** upon irradiation.[35,41] Additionally, we expected that after prolonged irradiation the tubes would completely disassemble. After a short period of irradiation (3 min), cryoTEM analysis (see the Supporting Information, materials and methods sections for experimental details) shows the appearance of gaps in the walls of the tubes while vesicles are still present within the nanotubes (Figure 4A). After 6 minutes of irradiation, shorter nanotubes

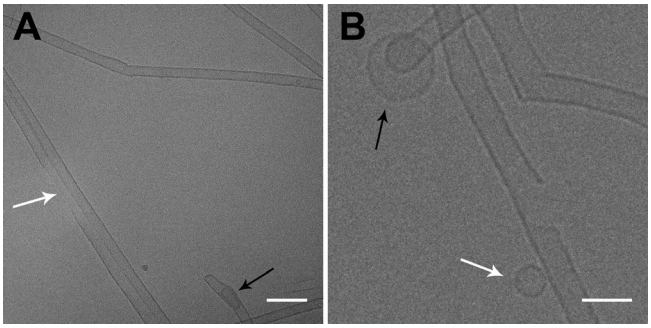

Figure 4. CryoTEM images of DOPC:**1** (1:1 w/w, 1 mg mL^{-1} each; in 10 mM aq. NaCl) to which a 200 mM aq. NaCl solution is added to induce the formation of vesicles inside the nanotubes. The sample was then irradiated at $\lambda = 365$ nm for A) 3 min and B) 6 min. In (A) the white arrow indicates a gap formed during irradiation and the black arrow indicates a vesicles still remaining inside the nanotube. In (B) the white arrow indicates a small vesicle released through a gap in the nanotube formed during the irradiation and the black arrow indicates a larger vesicle most probably present initially in the sample (see text for discussion). Scale bar in (A) = 100 nm, in (B) = 50 nm.

remain but included vesicles are not detectable (Figure 4B). We propose that the vesicles inside the nanotubes are released through the gaps in the nanotube bilayer walls caused by the irradiation with UV light, and can subsequently adopt a more favorable spherical geometry. It has to be noted that free DOPC vesicles are present in the sample before irradiation (Figure 3A) and it can therefore not be excluded that some of the vesicles, detected in the vicinity of the nanotubes after irradiation, are already present in the sample before irradiation and are not released from the inside of the nanotubes. However, the relatively small size of the vesicles (Figure 4B) in the immediate vicinity of the nanotubes with gaps in their walls correlates well to the sizes observed for vesicles included inside the nanotubes prior to irradiation (Section S1 in the Supporting Information). Moreover, no tubular or cylindrical vesicles can be detected after irradiation of the nanotubes, further supporting our hypothesis. Additional control studies demonstrated that DOPC vesicles were not affected by UV irradiation under hyperosmotic conditions (Figures S6, S7), ruling out that the vesicles themselves undergo changes during irradiation.

In conclusion, we have demonstrated in a multicomponent self-assembled nanosystem the use of osmotic pressure to incorporate vesicles initially attached to the end of an amphiphilic nanotube into the nanotube itself. Furthermore, it is shown that even a low salt gradient between the inside and outside of the capped nanotubes is sufficient to induce the inclusion of vesicles. A potential mechanism for the inclusion of vesicles into nanotubes is proposed and experimental evidence to support our hypothesis is obtained by electron

cryotomography. Additionally, it was demonstrated that the loaded nanotubes remain photoresponsive and the vesicles inside the nanotubes appear to be released upon irradiation.

The findings presented here offer an attractive opportunity to stabilize vesicles and design novel carrier systems. Vesicles are considered of major interest for targeted drug-delivery applications since they are nontoxic, biocompatible, and biodegradable.[42] A potential cargo can be either loaded into the hydrophobic part of the lipid bilayer of a vesicle or into the hydrophilic inside of the vesicle itself.[43] However, a disadvantage of the use of vesicles for drug delivery is their instability in vitro. Approaches to overcome this problem include the incorporation of polyethyleneglycol (PEG) chains onto the outside of the membranes of vesicles to increase the stability.[44] The nanotubes which encapsulate the vesicles will have PEG chains on their outer walls and might therefore contribute to enhancing the stability of vesicles inside the nanotubes. These responsive hybrid systems have potential to be applied in nanoscale, stimuli-responsive drug delivery. Studies along these lines are currently underway in our laboratories.

Acknowledgements

P.M.E. and L.S.v.B. acknowledge the Stichting voor Fundamenteel Onderzoek der Materie (FOM) for funding. Financial support from NanoNed, the Netherlands Organization for Scientific Research (NWO-CW), the European Research Council (Advanced Investigator Grant, No. 227897 to B.L.F.), the Ministry of Education, Culture and Science (Gravitation program 024.001.035), and the "Top Research School" program of the Zernike Institute for Advanced Materials under the Bonus Incentive Scheme (BIS) are gratefully acknowledged.

Keywords: amphiphiles · confined vesicles · nanostructures · osmosis · self-assembly

How to cite: *Angew. Chem. Int. Ed.* **2015**, *54*, 15122–15127
Angew. Chem. **2015**, *127*, 15337–15342

[1] a) J.-M. Lehn, *Science* **2002**, *295*, 2400–2403; b) R. F. Service, *Science* **2005**, *309*, 95.

[2] a) G. M. Whitesides, B. Grzybowski, *Science* **2002**, *295*, 2418–2421; b) S. G. Zhang, *Nat. Biotechnol.* **2003**, *21*, 1171–1178; c) L. Zhang, Y. K. Che, J. S. Moore, *Acc. Chem. Res.* **2008**, *41*, 1596–1608; d) L. C. Palmer, S. I. Stupp, *Acc. Chem. Res.* **2008**, *41*, 1674–1684; e) M. Yoshizawa, J. K. Klosterman, M. Fujita, *Angew. Chem. Int. Ed.* **2009**, *48*, 3418–3438; *Angew. Chem.* **2009**, *121*, 3470–3490; f) B. M. Rosen, C. J. Wilson, D. A. Wilson, M. Peterca, M. R. Imam, V. Percec, *Chem. Rev.* **2009**, *109*, 6275–6540; g) K. Matyjaszewski, N. V. Tsarevsky, *Nat. Chem.* **2009**, *1*, 276–288; h) N. C. Seeman, *Annu. Rev. Biochem.* **2010**, *79*, 65–87; i) Z. H. Nie, A. Petukhova, E. Kumacheva, *Nat. Nanotechnol.* **2010**, *5*, 15–25; j) M. Grzelczak, J. Vermant, E. M. Furst, L. M. Liz-Marzán, *ACS Nano* **2010**, *4*, 3591–3605; k) R. Chakrabarty, P. S. Mukherjee, P. J. Stang, *Chem. Rev.* **2011**, *111*, 6810–6918; l) Y. Mai, A. Eisenberg, *Chem. Soc. Rev.* **2012**, *41*, 5969–5985.

[3] a) J. A. A. W. Elemans, A. E. Rowan, R. J. M. Nolte, *J. Mater. Chem.* **2003**, *13*, 2661–2670; b) T. Aida, E. W. Meijer, S. I. Stupp, *Science* **2012**, *335*, 813–817.

[4] a) Y.-C. Yu, P. Berndt, M. Tirrell, G. B. Fields, *J. Am. Chem. Soc.* **1996**, *118*, 12515–12520; b) M. Li, H. Schnablegger, S. Mann, *Nature* **1999**, *402*, 393–395; c) M. Kwak, A. Herrmann, *Chem. Soc. Rev.* **2011**, *40*, 5745–5755; d) X. Yan, S. Li, T. R. Cook, X. Ji, Y. Yao, J. B. Pollock, Y. Shi, G. Yu, J. Li, F. Huang, P. J. Stang, *J. Am. Chem. Soc.* **2013**, *135*, 14036–14039.

[5] G. Cevc, *Phospholipids Handbook*, Marcel Dekker, New York, **1993**.

[6] a) T. Kunitake, *Angew. Chem. Int. Ed. Engl.* **1992**, *31*, 709–726; *Angew. Chem.* **1992**, *104*, 692–710; b) T. Shimizu, M. Masuda, H. Minamikawa, *Chem. Rev.* **2005**, *105*, 1401–1443; c) D. E. Discher, F. Ahmed, *Annu. Rev. Biomed. Eng.* **2006**, *8*, 323–341; d) C. Wang, Z. Wang, X. Zhang, *Acc. Chem. Res.* **2012**, *45*, 608–618.

[7] a) D. E. Discher, A. Eisenberg, *Science* **2002**, *297*, 967–973; b) P. Tanner, P. Baumann, R. Enea, O. Onaca, C. Palivan, W. Meier, *Acc. Chem. Res.* **2011**, *44*, 1039–1049.

[8] a) S. Jain, F. S. Bates, *Science* **2003**, *300*, 460–464; b) R. P. Brinkhuis, F. P. J. T. Rutjes, J. C. M. van Hest, *Polym. Chem.* **2011**, *2*, 1449–1462.

[9] a) J. D. Hartgerink, E. Beniash, S. I. Stupp, *Science* **2001**, *294*, 1684–1688; b) I. W. Hamley, *Soft Matter* **2011**, *7*, 4122–4138.

[10] a) J. Eastoe, A. Vesperinas, *Soft Matter* **2005**, *1*, 338–347; b) H. Oh, V. Javvaji, N. A. Yaraghi, L. Abezgauz, D. Danino, S. R. Raghavan, *Soft Matter* **2013**, *9*, 11576–11584.

[11] A. Ciesielski, C.-A. Palma, M. Bonini, P. Samorì, *Adv. Mater.* **2010**, *22*, 3506–3520.

[12] C. D. H. Alarcon, S. Pennadam, C. Alexander, *Chem. Soc. Rev.* **2005**, *34*, 276–285.

[13] a) S. Yagai, A. Kitamura, *Chem. Soc. Rev.* **2008**, *37*, 1520–1529; b) C. Park, K. Lee, C. Kim, *Angew. Chem. Int. Ed.* **2009**, *48*, 1275–1278; *Angew. Chem.* **2009**, *121*, 1301–1304.

[14] Y.-Z. You, C.-Y. Hong, C.-Y. Pan, P.-H. Wang, *Adv. Mater.* **2004**, *16*, 1953–1957.

[15] J. H. Gao, H. W. Gu, B. Xu, *Acc. Chem. Res.* **2009**, *42*, 1097–1107.

[16] P. V. Kamat, K. G. Thomas, S. Barazzouk, G. Girishkumar, K. Vinodgopal, D. Meisel, *J. Am. Chem. Soc.* **2004**, *126*, 10757–10762.

[17] L. M. Carrick, A. Aggeli, N. Boden, J. Fisher, E. Ingham, T. A. Waigh, *Tetrahedron* **2007**, *63*, 7457–7467.

[18] C. Lin, J. A. Ritter, *Carbon* **1997**, *35*, 1271–1278.

[19] K. S. Suslick, G. J. Price, *Annu. Rev. Mater. Sci.* **1999**, *29*, 295–326.

[20] a) S. F. Medeiros, A. M. Santos, H. Fessi, A. Elaissari, *Int. J. Pharm.* **2011**, *403*, 139–161; b) R. M. Choueiri, A. Klinkova, H. Thérien-Aubin, M. Rubinstein, E. Kumacheva, *J. Am. Chem. Soc.* **2013**, *135*, 10262–10265.

[21] a) D. Roy, J. N. Cambre, B. S. Sumerlin, *Prog. Polym. Sci.* **2010**, *35*, 278–301; b) F. D. Jochum, P. Theato, *Chem. Soc. Rev.* **2013**, *42*, 7468–7483.

[22] a) Y. Qui, K. Park, *Adv. Drug Delivery Rev.* **2001**, *53*, 321–339; b) J. J. D. de Jong, L. N. Lucas, R. M. Kellogg, J. H. van Esch, B. L. Feringa, *Science* **2004**, *304*, 278–281; c) X. Yan, T. R. Cook, J. B. Pollock, P. Wei, Y. Zhang, Y. Yu, F. Huang, P. J. Stang, *J. Am. Chem. Soc.* **2014**, *136*, 4460–4463.

[23] a) C.-Y. Lai, B. G. Trewyn, D. M. Jeftinija, K. Jeftinija, S. Xu, S. Jeftinija, V. S.-Y. Lin, *J. Am. Chem. Soc.* **2003**, *125*, 4451–4459; b) D. Tarn, C. E. Ashley, M. Xue, E. C. Carnes, J. I. Zink, C. J. Brinker, *Acc. Chem. Res.* **2013**, *46*, 792–801.

[24] a) M. Vallet-Regí, F. Balas, D. Arcos, *Angew. Chem. Int. Ed.* **2007**, *46*, 7548–7558; *Angew. Chem.* **2007**, *119*, 7692–7703; b) Z. X. Li, J. C. Barnes, A. Bosoy, J. F. Stoddart, J. I. Zink, *Chem. Soc. Rev.* **2012**, *41*, 2590–2605.

[25] a) M. A. C. Stuart, W. T. S. Huck, J. Genzer, M. Müller, C. Ober, M. Stamm, G. B. Sukhorukov, I. Szleifer, V. V. Tsukruk, M. Urban, F. Winnik, S. Zauscher, I. Luzinov, S. Minko, *Nat. Mater.* **2010**, *9*, 101 – 113; b) K.-Y. Chen, O. Ivashenko, G. T. Carroll, J. Robertus, J. C. M. Kistemaker, G. London, W. R. Browne, P. Rudolf, B. L. Feringa, *J. Am. Chem. Soc.* **2014**, *136*, 3219 – 3224.
[26] J. M. Hu, S. Y. Liu, *Macromolecules* **2010**, *43*, 8315 – 8330.
[27] a) M. De, P. S. Ghosh, V. M. Rotello, *Adv. Mater.* **2008**, *20*, 4225 – 4241; b) J. Robertus, W. R. Browne, B. L. Feringa, *Chem. Soc. Rev.* **2010**, *39*, 354 – 378.
[28] V. D. Gordon, X. Chen, J. W. Hutchinson, A. R. Bausch, M. Marquez, D. A. Weitz, *J. Am. Chem. Soc.* **2004**, *126*, 14117 – 14122.
[29] a) K. T. Kim, J. H. Zhu, S. A. Meeuwissen, J. J. L. M. Cornelissen, D. J. Pochan, R. J. M. Nolte, J. C. M. van Hest, *J. Am. Chem. Soc.* **2010**, *132*, 12522 – 12524; b) S. A. Meeuwissen, K. T. Kim, Y. Chen, D. J. Pochan, J. C. M. van Hest, *Angew. Chem. Int. Ed.* **2011**, *50*, 7070 – 7073; *Angew. Chem.* **2011**, *123*, 7208 – 7211.
[30] J. M. Morgan, *Annu. Rev. Plant Phys.* **1984**, *35*, 299 – 319.
[31] H. Lodish, A. Berk, S. L. Zipursky, P. Matsudaira, D. Baltimore, J. Darnell, *Molecular Cell Biology*, 4th ed., W. H. Freeman, New York, **2000**.
[32] a) R. Lipowsky, *Nature* **1991**, *349*, 475 – 481; b) U. Seifert, *Adv. Phys.* **1997**, *46*, 13 – 137.
[33] a) H. Hotani, *J. Mol. Biol.* **1984**, *178*, 113 – 120; b) T. van der Heide, M. C. A. Stuart, B. Poolman, *EMBO J.* **2001**, *20*, 7022 – 7032; c) M. Yanagisawa, M. Imai, T. Taniguchi, *Phys. Rev. Lett.* **2008**, *100*, 148102.
[34] N. S. Templeton, D. D. Lasic, P. M. Frederik, H. H. Strey, D. D. Roberts, P. M. Pavlakis, *Nat. Biotechnol.* **1997**, *15*, 647 – 652.
[35] A. C. Coleman, J. M. Beierle, M. C. A. Stuart, B. Maciá, G. Caroli, J. T. Mika, D. J. van Dijken, J. Chen, W. R. Browne, B. L. Feringa, *Nat. Nanotechnol.* **2011**, *6*, 547 – 552.
[36] T. Shimizu, M. Kogiso, M. Masuda, *Nature* **1996**, *383*, 487 – 488.
[37] a) S. M. Johnson, M. Buttress, *Biochim. Biophys. Acta Biomembr.* **1973**, *307*, 20 – 26; b) V. S. Malinin, P. Frederik, B. R. Lentz, *Biophys. J.* **2002**, *82*, 2090 – 2100; c) For a detailed analysis of bending and stretching deformations in vesicle membranes, see: R. Lipowsky, *Adv. Colloid Interface Sci.* **2014**, *208*, 14 – 24, and references therein.
[38] W. Baumeister, R. Grimm, J. Walz, *Trend Cell. Biol.* **1999**, *9*, 81 – 85.
[39] A tomographic slice is a section of the reconstructed 3D volume.
[40] The same color pattern for highlighting the various features in the tomogram has also been applied to Figure 3.
[41] a) W. R. Browne, M. M. Pollard, B. de Lange, A. Meetsma, B. L. Feringa, *J. Am. Chem. Soc.* **2006**, *128*, 12412 – 12413; b) A. C. Coleman, J. Areephong, J. Vicario, A. Meetsma, W. R. Browne, B. L. Feringa, *Angew. Chem. Int. Ed.* **2010**, *49*, 6580 – 6584; *Angew. Chem.* **2010**, *122*, 6730 – 6734.
[42] C. Chen, D. Han, C. Cai, X. Tang, *J. Controlled Release* **2010**, *142*, 299 – 311.
[43] O. P. Medina, Y. Zhu, K. Kairemo, *Curr. Pharm. Des.* **2004**, *10*, 2981 – 2989.
[44] A. L. Klibanov, K. Maruyama, V. P. Torchilin, L. Huang, *FEBS Lett.* **1990**, *268*, 235 – 237.

Received: July 14, 2015
Revised: August 17, 2015
Published online: October 27, 2015

